www.czasopisma.pan.pl PAN www.journals.pan.pl
POLSKA AKADEMIA NAUK

GEODESY AND CARTOGRAPHY
Vol. 67, No. 1, 2018, pp. 35–55

DOI: https://doi.org/10.24425/118701

Original research paper

Mobile Laser Scanning accuracy assessment for the purpose of base-map updating

Anna Fryskowska[1]*, Patryk Wroblewski[2]

[1,2]Military University of Technology
Faculty of Civil Engineering and Geodesy, Institute of Geodesy
Department of Remote Sensing, Photogrammetry and Imagery Intelligence
2 gen. W. Urbanowicza St. 00-908 Warsaw 46, Poland

[1]e-mail: anna.fryskowska@wat.edu.pl, ORCID: https://orcid.org/0000-0001-5449-8092
[2]e-mail: patryk_wroblewski95@wp.pl, ORCID: https://orcid.org/0000-0001-7181-6574

*Corresponding author: Anna Fryskowska

Received: 19 February 2018 / Accepted: 10 April 2018

Abstract: The aim of the research was to analyze the possibility of using mobile laser scanning systems to acquire information for production and/or updating of a basic map and to propose a no-reference index of this accuracy assessment. Point clouds have been analyzed in terms of content of interpretation and geometric potential. For this purpose, the accuracy of point clouds with a georeference assigned to the base map objects was examined. In order to conduct reference measurements, a geodetic network was designed and also additional static laser scanning data has been used. The analysis of mobile laser scanning (MLS) data accuracy was conducted with the use of 395 check points. In the paper, application of the total Error of Position of the base-map Objects acquired with the use of MLS was proposed. Research results were related to reference total station measurements. The resulting error values indicate the possibility to use an MLS point cloud in order to accurately determine coordinates for individual objects for the purposes of standard surveying studies, e.g. for updating some elements of the base map content. Nevertheless, acquiring MLS point clouds with satisfying accuracy not always is possible, unless specific resolution condition is fulfilled. The paper presents results of accuracy evaluation in different classes of base-map elements and objects.

Keywords: mobile Laser Scanning, base-map, data accuracy

---

1. Introduction and related works

Mobile laser scanning (MLS) is an integrated system of many sensors, including navigation devices and devices for collecting spatial data, mounted on a platform that has the ability to move (usually a car) and acquire data along the route (Kaartinen et al., 2012; Mikrut et al., 2016). Currently remote sensing sensors, like airborne and terrestrial LIDAR, RADAR and scanners, are able to collect high density data of the Earth surface or terrestrial objects (Jenerowicz and Siok, 2017; Bobkowska et al., 2016; Glowienka et al., 2017). Also, terrestrial lidar data can be use itself for accuracy determination of other data (Woroszkiewicz et al. 2017; Markiewicz and Zawieska, 2015; Lubczonek, 2016; Wilinska et al., 2012; García and Lerma, 2013 or Fryskowska et al., 2015).

Data from laser scanning systems enable the measurement of hundreds of thousands of points per second. Data is collected in the form of a point cloud reflecting all objects encountered. In geodetic processes, in particular the construction of a basic map with classical methods, individual objects or points representing them are measured. Despite the measurement system, the most valid and final indication of the data quality is given by the accuracy, the degree of agreement between a measurement and the conventional true value of the quantity being measured (Iavarone, 2002).

The aim of the work was to analyze the possibility of using laser scanning systems to acquire information for creating and/or updating of a basic map. Point clouds have been analyzed in terms of object identification and geometric potential. For this purpose, the accuracy of point clouds with a georeference assigned the base map objects was examined.

The subject of accuracy of such LIDAR data is actual in many research. The publications: (Bakula et al., 2015; Lenda et al., 2015; Kedzierski et al., 2015; Zacharek et al., 2017 and Lichti et al., 2005) are focused on accuracy assessment of laser scanner data in different applications: surface modelling, scan registration, data fusion, archaeology or architecture.

The subject of direct georeferencing of point clouds is currently one of the most important directions of work on improving both static and mobile laser scanning systems and is often undertaken in literature (Reshetyuk, 2010; Shan and Toth, 2009; Osada et al., 2017; Lichti et al., 2005; Fryskowska, 2017; Santos et al., 2013 or Scaioni, 2005). Nevertheless accuracy analysis of mobile laser scanning data requires specific approach, including georeferencing component.

Various methods and approaches to the problem of the accuracy analysis of the data obtained with mobile laser scanning can be found in the literature. The differences between those methods consist mainly in the parameters that are calculated in order to assess data accuracy. Some authors choose advanced statistical methods, which are based on the assumption that residuals at certain points in MLS are characterised by the occurrence of the normal distribution. These methods, proposed in publications such as (Toschi et al., 2015), lead to the calculation of the mean value, median, standard deviation, and parameters that allow to determine the occurrence of potential asymmetries in the distribution of residuals from the mean value and the occurrence of residuals distribution in the form of a low and wide Gaussian curve or a high and narrow Gaussian curve. There are also methods that are based only on error analysis (Kaartinen et al., 2012). Another difference in the approach to the conducted accuracy analysis is based on the type of reference data used. Authors use data obtained by means of tachymetry, static terrestrial laser scanners, and GPS RTK receivers; for example, the authors of (Poreba and Goulette, 2012) for reference data used the data obtained by means of both total station and static terrestrial laser scanners, while the authors of (Gandolfi et al., 2008) used only the results of GPS RTK measurements as reference data.

The authors of publications such as (Kaartinen et al., 2012; 2013) conducted accuracy analyses for various mobile laser scanning systems, later comparing them, determining the level of horizontal and vertical accuracy that could be reached with the use of each of these systems. These studies were conducted as part of the European Spatial Data Research (EuroSDR) concerning data obtained from mobile platforms. The following MLS systems were analysed: ROAMER, Riegl VMX-250, Sensei, StreetMapper 360, and Optech Lynx. Based on the root mean square errors of the horizontal points ($RMSE_{XY}$), compared by the authors of (Kaartinen et al., 2012; 2013), it was determined that the lowest horizontal error was obtained for the ROAMER and Riegl VMX-250 systems ($RMSE_{XY} = \pm 0.020$ m), while the highest horizontal error was obtained for the Optech Lynx system ($RMSE_{XY} = \pm 0.043$ m). For other MLS systems, horizontal error values are in the range determined by the set boundary (maximum) values. This means that in terms of the accuracy of the horizontal position of points, there are no significant discrepancies between the different MLS systems, and all the systems analysed by the authors of (Kaartinen et al., 2012; 2013) are characterised by the possibility of obtaining data with high horizontal accuracy (with errors in the range of a few centimetres). Regarding the assessment of altitude accuracy, the authors of (Kaartinen et al., 2012; 2013) did not provide RMS error values for the heights of points, but used the obtained maximum values of altitude residuals and the values of standard deviations. (Kaartinen et al., 2013) draw attention to the fact that one of the basic factors affecting the accuracy of mobile laser scanning data is the GNSS signal quality. In the conditions of good communication with satellites, the authors obtained horizontal accuracy at the level of 30 mm for one of the point clouds analysed, while in the case of strong interferences this accuracy deteriorated, and the errors obtained oscillated around 1 m. The accuracy of the horizontal position and the altitude of points in a point cloud obtained from mobile laser scanning determines the possibility of using MLS data for some standard geodetic applications (e.g. updating the base map.)

So far, the analyses have focused on the assessment of accuracy in relation to other photogrammetric and total station data. The present article aims to determine the absolute accuracy of MLS data, taking into consideration different parameters and aspects of these point clouds.

2. Data and study area

The analysis uses the data from static topographic terrestrial laser scanner and mobile topographic terrestrial laser scanner, covering the same study area. The works were carried out in the urban area of the city of Warsaw (Poland). The test areas have been selected to cover various types of objects. In test area 1 there are a large number of objects constituting the content of the base map: building corners, pavement curbs, road curbs, trees, sewage manholes, sewage grates, rectangular manholes, lamp posts, hydrants; as well as objects not constituting the content of the base map but clearly determinable: window corners, roof corners, etc. (Figures: A1 and A2). Test areas 2 and 3 were selected due to the fact that these are areas in which mainly buildings are located. The objects are buildings with a simple construction. The roofs are flat (or close to flat), they have an uncomplicated shape, but with numerous simple elements located on the roof and façade of the buildings. Figure 1 shows the location of the selected areas.

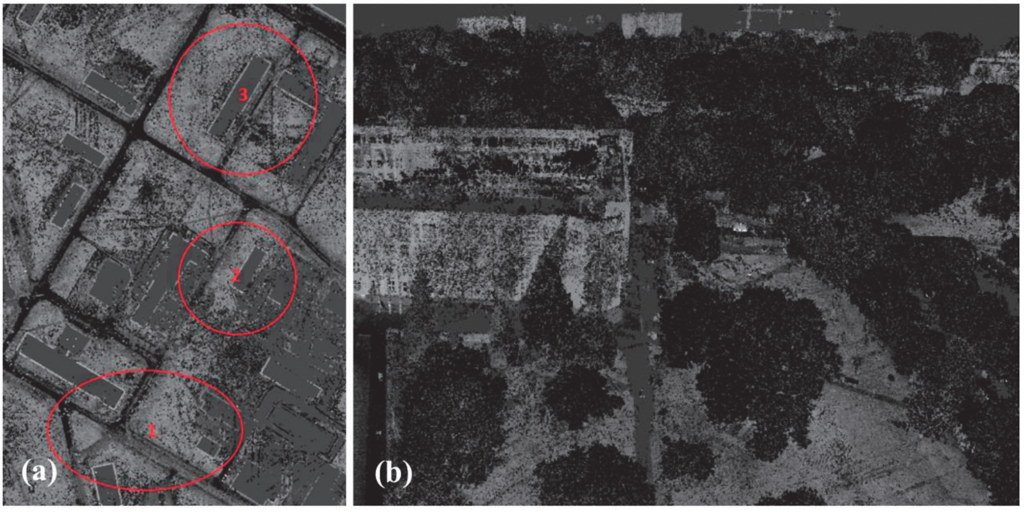

Fig. 1. Chosen test areas: a) MLS data top view, b) fragment of MLS test area

The data for analyzes was acquired using Leica ScanStation2 terrestrial laser scanner and Trimble MX8 mobile laser scanner. Additionally, for reference measurements total station has been used.

The Leica ScanStation 2 impulse scanner has the accuracy of a single distance measurement of ±4 mm, the accuracy of a single position measurement of ±6 mm, the accuracy of horizontal and vertical measurements of ±60 microradians and HDS target scanning error of ±2 mm. The range of this scanning device is up to 300 m with 90% albedo and 134 m with 18% albedo. Data from static laser scanner have been transformed on the basis of 16 reference points, constituting situational details (corners of roofs, windows, etc.), to the systems: PL-2000 and PL-EVRF-2007-NH. Georeferencing accuracy gained ±0.024 m.

The Riegl VMX-250 MLS system comprises two Riegl VQ-250 laser scanners, which are calibrated and integrated with a high-precision inertial measurement unit/ global navigation satellite system (IMU/GNSS) pose/positioning module and a Riegl software package for data post-processing (Figure 2).

The scanner has a laser beam divergence of 0.36 mrad and can run high-performance pulsed ranging with high penetrability through obstructions (e.g., plants and fences). System is characterized by the accuracy of distance measurement of 10 mm (at a distance of about 50 m), and the positioning accuracy of the GNSS / IMU system is 20–50 mm (Lin et al., 2013).

A Topcon GPT-3107N reflectorless instrument was used to set a geodetic control network and reference surveying measurements (20^{cc} angle accuracy, ±2 mm + 2ppm

Fig. 2. System MSL Riegl VMX-250 (N3)

– distance accuracy) and Leica Sprinter 250M code leveler (with an error of 0.7–1.0 mm per 1 km of traverse) (N1, N2).

2.1. Reference data

In order to conduct reference measurements, a network was designed, consisting ten points of geodetic measurement network (P1–P10), tied to five points of the national control network (W102, W103, W104, W106, W107). The horizontal network points were fixed. Next, a vertical network was designed in order to conduct vertical tying on at least two vertical benchmarks. As a result, a levelling line was created, consisting of two vertical tie points (Rp104, Rp106) and seventeen created points of surveying vertical network (Rpr0, Rpr1, Rpr2, Rpr2A, Rpr3, Rpr4, Rpr5, Rpr6, Rpr7, Rpr8, Rpr9, Rpr10, Rpr11, Rpr12, Rpr13, Rpr14, Rpr15). The geodetic measurement network points were fixed on the surface of permanent terrain details, such as pavement curbs or concrete castings around sewer manholes located on the roadside. With the points of both the horizontal and vertical networks ready and fixed in the field, the next stage of the work was to measure the horizontal and vertical networks. The adjustment of the linear-angular network was carried out in the C-GEO software. As a result of the rigorous adjustment of the linear-angular network, the adjusted coordinates of the points of the geodetic measurement network were obtained, where the majority of the points is characterised by a position error (2D) at the level of ±5–8 mm with maximum value of ±12 mm. Due to the fact that the length of the traverse was about 0.815 km, the permissible value of the residual for each traverse was about ±18 mm. Having prepared a horizontal and vertical measurement networks, it was possible to measure the tachymetric situational details, which were to be later used as reference points for the assessment of MLS data accuracy and enable the georeferencing of the scans obtained with static terrestrial laser scanners (Appendix 1).

The accuracy of reference points determination is up to 10 mm (2D) and 20 mm (3D) related to geodetic network. For further analysis, geodetic network points are considered as a correct.

The measurements were also referred to other terrestrial pulse laser scanning system in the context of accuracy comparison. However, in the next part of the article, they will not be considered as being used for geodetic works, only to be used as a comparison MSL data.

3. Methods and workflow

The data used for the analysis was oriented to the same national geodetic reference frame. Reference data for the accuracy assessment consisted of total station measured points on selected objects. The points analysed within the overall MLS accuracy assessment were divided into object classes, depending on what real-world object they represent; next, root mean square errors for each class were determined. Dividing the analysed objects into classes and calculating the horizontal and vertical accuracy for each class was aimed at determining the suitability of using MLS for obtaining data on the location of specific objects in space.

Laser scanning data accuracy was assessed in terms of the quality of identification of characteristic elements in the point cloud. This quality is understood both as geometric accuracy and the unambiguous determination of the location of the selected point.

When comparing point clouds acquired by different instruments, some issues should be considered: its own sources of uncertainties and sensitivity to outlier presence, the compared 3D points are not exactly corresponding to each other and the object surfaces are not equally digitized as the acquisition positions are different (Toschi et al., 2015).

Taking into consideration these factors, some other, additional elements were included in this research. Generally, Lichti and Gordon in (Lichti and Gordon, 2004) imply classify the errors in TLS into two groups: *internal* (instrumental in our case) and *external* (here one might include object-related, environmental and georeferencing errors, according to our classification). There are many other classifications, but for MLS quality assessment in geodetic applications in terms of detection and identification of elements, the following aspects and classes are the most important:

i) accuracy of spatial coordinates influenced by inner, instrumental error – A_{IA},
ii) scan/point cloud interpretative resolution error – A_{RES},
iii) orientation of point clouds from different positions or/and georeferencing error – A_{GEO},
iv) completeness (missing data, occlusions etc.) accuracy – A_{COM},
v) homogeneity towards reference data accuracy – A_{HOM}.

The aim of this work is to propose a new mobile laser scanning accuracy index (OPE_{MSL}). It would be helpful to no-reference accuracy assessment of mobile laser scanning data and its application in base-map actualization purposes.

Generally, the total Error of Position of the base-map elements/Objects acquired with the use of MLS – can be considered as function of these factors:

$$OPE_{MSL} = f(A_{IA}, A_{RES}, A_{GEO}, A_{COM}, A_{HOM}) \tag{1}$$

For further analysis in this paper, completeness A_{COM} and homogeneity towards reference data A_{HOM} are omitted. This research is related to geometric potential of MSL in base map creation, so for this analysis we consider these factors as fulfilled.

In further subsections, the first three accuracy components are described.

3.1. Instrumental and georeferencing errors – A_{IA} *and* A_{GEO}

Inner instrumental accuracy (A_{IA}) depends on instrumental potential and are attributable to the scanner design. These errors can be fundamental (inherent to the physics of laser range finder) and errors specific to the scanner hardware, including the laser rangefinder, beam deflection unit, angle measurement system and axes errors. These errors can be potentially removed or minimized by improving the system design, or by calibration (Reshetyuk, 2009; Herbert and Krotkov, 1992). Instrumental errors have both random and systematic influences on the laser scanning measurements. For purposes of presented research instrumental error represent the accuracy of determination of single point in the cloud.

Table 1 presents brief specification of instruments used in this research (the Riegl VMX-250, and Leica ScanStation2) and for comparison two other systems (Roamer and FARO). The Roamer MLS system adopts a FARO LS 880HE80 laser scanner for 3D mapping, with its spatial trajectory derived by the NovAtel SPAN (Synchronized Position Attitude Navigation) technology and FARO FOCUS 3D is a static-phase scanner. The indirect georeferencing of static scanners can differ in accuracy. It is dependent on transformation accuracy and for geodetic applications not should exceed 0.10 m.

Table 1. Specifications of mobile and static laser scanning – (on the basis of (Lin et al., 2013), (N4) (N3))

	Riegl VMX-250	Roamer	ScanStation2	FaroFocus
Ranging accuracy [mm]	10 @ 50 m	20 @ 50 m	4 @ 50 m	3 @ 25 m
Point position accuracy [mm]	15	20	6	4
Georeferencing [mm]	20–50	20–50	20–60	20–60

For further analysis – A_{IA} will be considered as a single point position accuracy (table 1) and A_{GEO} as a georeferencing error.

These both errors are related to instrumental accuracy and Authors propose considering them as a general mobile laser scanning system error A_{SYS}:

$$A_{SYS}^2 = A_{IA}^2 + A_{GEO}^2 \tag{2}$$

3.2. Scan/point cloud interpretative resolution error – A_{RES}

Density and scan resolution – these are terms for defining how many points represent some surface of the scanned object. Point cloud resolution named as – density (expressed in points per square meter) or resolution ***Res*** (understand as an average distance between points) – is one of the most important factors that determine the accuracy of the coordinates of a point in the cloud. It can be determined in a different way. Here, to determine the average distance between the measurement points, the Delaunay triangulation algorithm was used. Delaunay's triangulation provides such a topological relationship between individual points that each of them has a strictly defined neighbour. The TIN building algorithm has been presented in detail in (Lee and Schachter, 1980 or Sloan, 1987). Figures 3(a) and 3(b) show a fragment of the TLS point cloud (a) and the resulting TIN (b) grid.

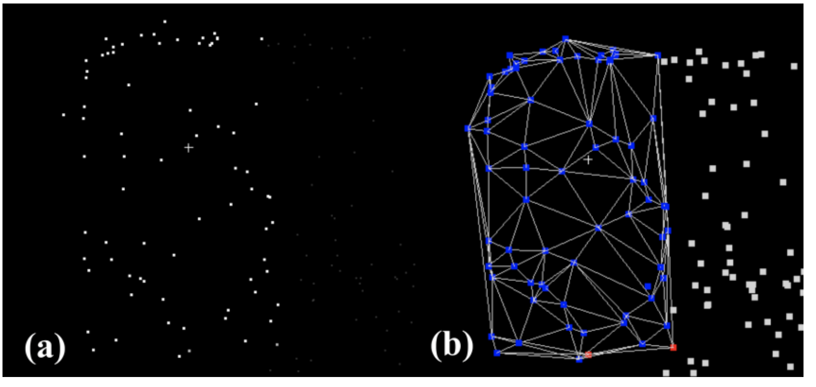

Fig. 3. (a) a fragment of the TLS point cloud, (b) the resulting TIN mesh

With reference to mobile laser scanning, resolution analysis was performed on objects that were inside the test areas. The analysis covered the walls of buildings (including window niches, doors, window sills, softs, etc.) and elements of road infrastructure (streets, pavements, curbs, sewage manholes, rectangular manholes, sewage grates, lamps). The comparison of average resolutions obtained for various objects on which the analysis were carried out is presented in Table 2.

Table 2. Mean values of MLS resolution in different test elements and areas

Object	Mean resolution *Res* [mm]
Facade 1 (road side)	20
Fasade 2	53
Side facade 1	38
Side facade 2 (road side)	36
Facade 3	52
Facade 4 (road side)	32
Road infrastructure (pavements, pawns, sevage manholes etc.)	13

It can be seen from Table 2 that these resolutions differ significantly. The highest average resolution was 13 mm, while the lowest was 53 mm. That means that the probability of indicating the correct element representing a given object will be about four times better in the case of an area where the resolution was 13 mm compared to the area where it was 53 mm due to the fact that points are located there at much smaller distances between each other, facilitating the interpretation of objects. Based on screen shots Figure 4(a) and 4(b) shows how the areas with higher and lower resolutions look visually.

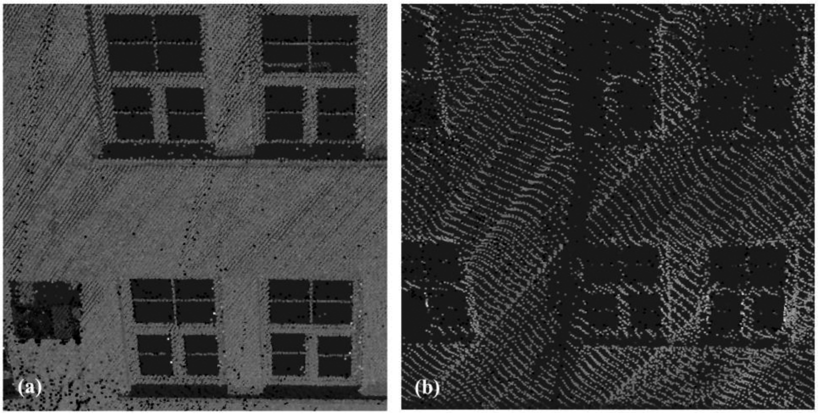

Fig. 4. MLS point clouds: (a) 20 mm resolution, (b) 53 mm resolution

Based on Figure 4, we can see how much the resolution affects the interpretation possibilities, and therefore the choice of points that represent a given object (e.g. a window corner) in fact. Already at this stage, it was noticeable that data from MLS will be characterized by varying accuracy in relation to various objects. The wall shown in Figure 4(a) was located in the immediate vicinity of the road (a few meters distance) constituting the route of the platform from the MLS. In addition, this wall was not covered by trees as much as the wall shown in Figure 4(b), which in addition to a very large number of trees growing a few meters away, was scanned from a considerable distance (several dozen meters). Thus, at this stage of the work, two factors have been noted, which due to lower resolution, also cause a decrease in the accuracy of data obtained from MLS: an increase in scan distance and the presence of a significant number of obstacles between the moving laser scanner and the scanned object.

After triangulation, the length of the triangle arms and their average values were calculated.

After elimination of gross errors (triangles on the edge of the object), the average distances between neighbouring points were obtained, respectively for TLS: 18 mm and MLS: 13–56 mm.

3.2.1. Resolution and interpretation

OPE_{MSL} mainly depend on point cloud resolution/density. Nevertheless, contains also the information about interpretative potential. This situation explains Figure 5.

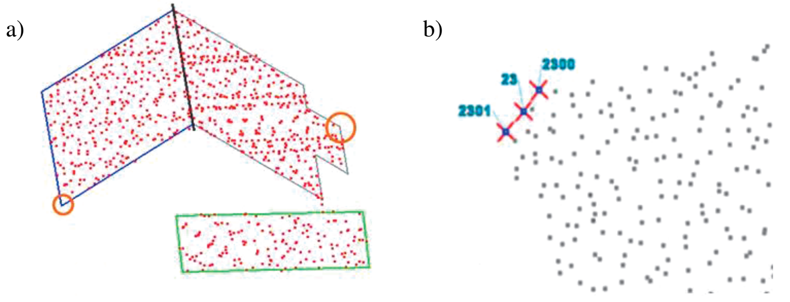

Fig. 5. Manual (a) and automatic (b) method of point identification

When defining a point in the cloud, which is to represent a given object (e.g. roof corner), we can use automatic or manual methods. In the case of the first of them, the point representing the corner can be a virtual point resulting from interpolation (Figure 5(a)) and in the case of the second method, it is necessary to select one of the points assumed for the potential reflection of the object (Figure 5(b)). In both cases, the resolution itself is not synonymous with an error of interpretation. Because the resolution itself does not take into account the interpretation capability of the point cloud, for further considerations below the formula will be used:

$$A_{RES} = \sqrt{2} \cdot Res \tag{3}$$

where *Res* is the nominal resolution of the point clouds expressed in [mm].

3.3. Preliminary accuracy assessment

Field measurements of check points were used for the preliminary analysis of the accuracy of data obtained by laser scanning. Distances between selected points (e.g. roof edges) and the approach to the analysis of individual points were determined.

The lengths of the roof edge were based on the total station measurement of spatial coordinates of the roof vertices (accuracy $\pm 3-5$ mm), while other elements of the building, such as window openings, stairs, etc. were measured with rule (accuracy ± 2 mm).

Check points selected for analysis had to meet the criteria of unambiguity and possibility of identification. Presented in Table 3 are the lengths of selected sections on the façade of a selected building, measured by means of total station measurements (TS) and cloud points from pulsed (IS) and mobile (MS) terrestrial laser scanners, as well as absolute values of length differences in relation to total station measurements.

Static terrestrial laser scanner (IS) was also used as a comparison of the same kind of data (mobile and static terrestrial laser scanning systems give point clouds, contrary to total station point measurements).

Based on the analyses performed, it can be concluded that the largest difference between the total station measurements and those obtained by means of a scanner occurs

Table 3. The results of length measurements and absolute values of the length differences of selected sections in relation to reference measurements

Section no.	|TS−IS| [m]	|TS−MS| [m]
1	0.016	**0.103**
2	0.009	**0.036**
3	**0.054**	**0.058**
4	0.017	**0.073**
5	0.008	**0.067**
6	0.022	**0.090**
7	0.029	**0.046**
8	**0.032**	**0.035**
9	0.011	0.002
Mean	**0.022**	**0.056**

with MS data. This is due to both the average distance between the points in a cloud and the method of obtaining them (navigational systems error). In the case of the other system, the average difference was ca. 20 mm. Distance differences exceeding the highest value of 30 mm are marked in bold type and are characteristic mainly for MS data.

3.3.1. Object Position Error of MLS data in geodetic applications

For the applications of the MLS accuracy analysis in base maps, only the first three aspects of formula 1 were considered, with the assumption that only complete and unambiguous data was analysed. Therefore, based on the conducted work, the following formula and the weights of each component influencing the resulting geometric accuracy OPE_{MSL} were determined:

$$OPE_{MLS}^2 = A_{SYS}^2 + A_{RES}^2 \tag{4}$$

Based on the above components, it is possible to determine the ultimate, estimate accuracy of already conducted MSL measurements. The accuracy was tested empirically with the specifications for natural, real scanning conditions, with changing atmospheric and lighting conditions, and not always favourable or exactly known conditions for obtaining data (angle, distance, resolution).

4. Results and discussion

The analysis of MLS data accuracy was conducted with the use of 395 check points and for TLS with the use of 159 check points. Not all points were used for the analysis of height accuracy, as in the case of some objects it resulted impossible to accurately determine the height (obscuring by other elements). It was assumed that total station measurements are real values and it was in relation to them that residuals of coordinates and heights of MLS points were calculated. The results are presented in Table 4. All values of calculated $RMSE_X$, $RMSE_Y$, $RMSE_H$ presented in following tables are expressed with millimetre precision. Of course, in base-map production such precision is not required. Usually, centimetres are used. Nevertheless, in this paper higher precision due to reference measurements and calculation procedure is applied.

Table 4. *RMSE* values for point location in point cloud from Mobile and Terrestrial Laser Scanning

	$RMSE_X$ [m]	$RMSE_Y$ [m]	$RMSE_H$ [m]	$RMSE_{XY}$ [m]
Mobile Laser Scanning	±0.040	±0.044	±0.042	±0.060
Terrestrial Laser Scanning	±0.023	±0.022	±0.016	±0.031

For every point analysed, residuals of the X coordinate, Y coordinate, and H height were calculated, as well as the point position error mP_i, as a function of the obtained residuals for X, Y, and H coordinates.

$$mP_i = \pm\sqrt{dX_i^2 + dY_i^2} \tag{5}$$

where: mP_i – position error of the i-th point in a set of points; dX, dY – residual of the X and Y coordinates of the i-th point in a set of points.

The percentage distribution of horizontal position errors of points (X, Y) in the entire data set was also determined in the ranges: $mP_i \leq RMSE_{XY}$, $RMSE_{XY} < mP_i \leq 2RMSE_{XY}$, $2RMSE_{XY} < mP_i \leq 3RMSE_{XY}$, $3RMSE_{XY} < mP_i \leq 4RMSE_{XY}$ and vertical residuals of points (the calculations used absolute values of vertical residuals) in the entire data set in ranges: $|dH_i| \leq RMSE_H$, $RMSE_H < |dH_i| \leq 2RMSE_H$, $2RMSE_H < |dH_i| \leq 3RMSE_H$, $3RMSE_H < |dH_i| \leq 4RMSE_H$. The results of these analyses are presented in Tables 5 and 6.

Table 5. The percentage distribution of horizontal position errors of points related to $RMSE_{XY}$ for MLS data

Range	Number of points	Percentage distribution in entire data set [%]
$mPi \leq RMSE_{XY}$	247	62.4
$RMSE_{XY} < mP_i \leq 2RMSE_{XY}$	146	37.0
$2RMSE_{XY} < mP_i \leq 3RMSE_{XY}$	1	0.3
$3RMSE_{XY} < mP_i \leq 4RMSE_{XY}$	1	0.3

Results in tables 5 and 6 show that values of mPi ranges according to Gaussian distribution. Based on the above, it can be concluded that 62.4% of points are characterised by a horizontal position error not exceeding the $RMSE_{XY}$ value (±0.060 m). For 37.0%

Table 6. The percentage distribution of vertical residuals of points' $|dH_i|$ related to $RMSE_H$ for MLS data

Range	Number of points	Percentage distribution in entire data set [%]
$\lvert dH_i \rvert \leq RMSE_H$	259	68.6
$RMSE_H < \lvert dH_i \rvert \leq 2RMSE_H$	105	27.9
$2RMSE_H < \lvert dH_i \rvert \leq 3RMSE_H$	10	2.7
$3RMSE_H < \lvert dH_i \rvert \leq 4RMSE_H$	3	0.8

of points, horizontal position errors are greater than $RMSE_{XY}$, but less than or equal to twice the $RMSE_{XY}$ value. Only in the case of two points have the mPi errors exceeded the threshold of double the $RMSE_{XY}$ value (in the case of one of these points, the $RMSE_{XY}$ value was exceeded three times). The maximum error value of the horizontal position error for the mP_i point was ± 0.23 m. It should be noted that 390 points (98.7% of the point set) is characterised by the horizontal position error of less than ± 0.10 m, which means that 98.7% of the points meet the accuracy requirements for the 1st accuracy group for situational details, as per the Regulation (Regulation in BM, 2011).

The Regulation defines three precision groups: for 1st, 2nd and 3rd precision group of situational details, the impassable horizontal errors of the position of the point (X, Y) with respect to the nearest horizontal points of the geodetic network are 0.10 m, 0.30 m, 0.50 m.

The obtained results indicate that the analysed data from mobile laser scanning is characterised by high horizontal accuracy, enabling its use, among others, for updating base maps.

4.1. Accuracy analysis within object classes

Given the fact that in order to analyse the accuracy of MLS point clouds, points that represented different real-world objects were used, all analysed points were divided into object classes and then the mean square root errors of horizontal position ($RMSE_{XY}$) and square root mean errors of height ($RMSE_H$) were calculated for each class.

Distinguished among the points subjected to accuracy analysis can be points representing objects that constitute the content of the base map (e.g. road curbs, pavement curbs, sewage manholes, rectangular manholes, sewage grates, building corners, lamp posts, trees, hydrants, and other permanent and characteristic elements of land development) and points representing other objects, analysed due to the fact that their shape allowed them to be unambiguously indicated on the point cloud from mobile laser scanning.

A total of 18 object classes were created: characteristic height elements (masts), trees, additional elements (all objects that were difficult to assign to separate classes, e.g. intersections of window grilles, air conditioning devices mounted on building walls), hydrants, sewage grates and their elements, pavement curbs, lamp posts, building corners, roof corners, windows, window sills, road cross-sections, gutters, stairs, posts, sewer manholes and their elements, streets/road curbs, rectangular manholes and their elements. The results of these calculations are presented in Table 7.

Table 7. The 18 object classes: *RMSE* and OPE_{MSL}

Object class	Number of test measurements	$RMSE_X$ [m]	$RMSE_Y$ [m]	$RMSE_H$ [m]	$RMSE_{XY}$ [m]	$RMSE_{XYH}$ [m]	OPE_{MSL} [m]
characteristic height el. (masts)	3	±0.050	±0.035	±0.025	±0.060	±0.065	**±0.062**
trees	49	±0.071	±0.080	±0.040	±0.110	±0.117	**±0.140**
additional elements	19	±0.040	±0.042	±0.050	±0.060	±0.078	**±0.700**
hydrants	3	±0.040	±0.063	±0.004	±0.080	±0.080	**±0.074**
sewage grates	12	±0.032	±0.032	±0.013	±0.045	±0.047	**±0.045**
pavement curbs	20	±0.040	±0.043	±0.015	±0.060	±0.062	**±0.066**
lamp posts	15	±0.040	±0.050	±0.040	±0.061	±0.073	**±0.081**
building corners	23	±0.040	±0.046	±0.073	±0.061	±0.095	**±0.088**
roof corners	18	±0.044	±0.064	±0.052	±0.080	±0.095	**±0.090**
windows (corners)	183	±0.040	±0.043	±0.050	±0.060	±0.078	**±0.060**
window sills	15	±0.034	±0.070	±0.060	±0.080	±0.100	**±0.130**
road cross-sections	8	±0.054	±0.030	±0.060	±0.061	±0.086	**±0.092**
gutters	16	±0.032	±0.051	±0.020	±0.060	±0.063	**±0.060**
stairs	8	±0.050	±0.011	±0.043	±0.050	±0.066	**±0.070**
posts	11	±0.032	±0.020	±0.012	±0.040	±0.042	**±0.050**
sewer manholes	15	±0.033	±0.033	±0.018	±0.050	±0.053	**±0.055**
streets/road curbs	34	±0.035	±0.041	±0.026	±0.053	±0.059	**±0.061**
rectangular manholes	10	±0.040	±0.034	±0.020	±0.051	±0.055	**±0.050**

In addition to the *RMSE* value, the OPE_{MSL} error values are also listed (bolded). They were calculated for all classes separately, referring to the resolutions in which individual elements occurred. The calculations were made on the same data sample as RMS errors.

The majority of object classes are characterised of a horizontal accuracy of ±0.060 m. The smallest accuracy was noted in the “trees” object class. However, it should be noticed that the conducted accuracy analysis refers the values read from the MLS point cloud to the total station measurements. In the case of trees, it is usually impossible to indicate the exact same point for tachymetric and MLS measurements due to the lack of unambiguous characteristic details. Thus, points representing trees were excluded from the accuracy analysis of the entire MLS point cloud. They were treated as a separate object class. As those details, according to the Regulation (Regulation in BM, 2011), belong to the 3rd accuracy group for situational details, their horizontal position must be determined with an error not greater than ±0.50 m. This means that the root mean square error of the horizontal position within this class is within the limit.

The values listed in the last column of Table 7, referring to the horizontal accuracy of point position ($RMSE_{XY}$), indicate that for all object classes, the accuracy requirements defined by the limit values for three accuracy groups for situational details were met. For all object classes, except the "trees" class, the obtained horizontal position errors were within the limits adopted for the 1st accuracy group for situational details. In the case of trees, the error value for the $RMSE_{XY}$ was higher, but since the trees are classified within the 3rd accuracy group, the error is within the acceptable limits.

The OPE_{MSL} values are close to the $RMSE$ values calculated on the basis of reference measurements. This shows the convergence of the results of both methods of accuracy evaluation. The advantage of the developed accuracy index is the ability to determine it without reference measurements, knowing the system parameters and the resulting point clouds.

The resulting error values indicate the possibility to use an MLS point cloud in order to accurately determine right-angle coordinates for individual objects for the purposes of standard surveying studies, e.g. for updating some elements of the base map content.

It should be noted that the base map is an example of a planimetric and contour map. This means that apart from accurate information on the horizontal position of points, the base map includes also information on the height of the represented objects. In order to determine whether it is possible to use the height of points obtained from an MLS point cloud as part of standard surveying studies, e.g. for updating the base map, the obtained root mean square error values for heights ($RMSE_H$) were also analysed and presented in Table 7.

The highest height error ($RMSE_H$) was noted for the "building corners" class, with the value of ±0.073 m. This error value was due to i.a. inaccessibility of a given element, in which case the lowest visible point was measured. This caused an increase in the $RMSE_H$ value for this object class. However, it should be noted that in situations where it was possible to measure a point on ground level, the horizontal residuals obtained were even two times lower than the $RMSE_H$ value obtained for the "building corners" class as a whole.

The lowest $RMSE_H$ value was obtained for the "hydrants" object class, with the error value of ±0.004 m. During the total station measurement, the highest point of a hydrant was measured, so it was possible to unambiguously indicate the corresponding point in the case of a point cloud.

In the case of the following object classes: characteristic height elements (masts), sewage grates, pavement curbs, gutters, roadside posts, sewer manholes and their elements, streets/road curbs, and rectangular manholes and their elements, root mean square errors obtained were at the level of $RMSE_H = \pm 0.010–0.030$ m. In the case of characteristic height elements (masts) and gutters, it is possible to indicate the highest points belonging to these objects. Other abovementioned objects (sewage grates, pavement curbs, roadside posts, sewer manholes and their elements, streets/road curbs, rectangular manholes and their elements) can be included in the set of road infrastructure objects. This means, in practice, that for road infrastructure objects the MLS point cloud is characterised by vertical accuracy at the level of ±0.010–0.030 m. This stems from the fact that these objects are situated either en route or in the immediate vicinity of the route of the platform with the MLS system installed. The relatively small scanning distance and the fact that there are usually no obstacles between the laser scanning beam and the scanned objects make it possible to obtain points representing road infrastructure objects with low vertical errors.

It should be noted that among the objects belonging to different classes, there can also be distinguished objects that differ significantly in terms of accuracy. It is exemplified i.a. by sewer manholes: mean vertical accuracy of the set of points representing sewer manholes and their elements was ±0.018 m (Tables 7 and 8). The measured manholes included both those located on the roads, the covers of which were at the level of the asphalt (in this case the vertical residuals obtained were at the level of a few millimetres), as well as manholes located at a great distance from the roads, in grassy areas, protruding ca. ±0.010–0.020 m above ground level (in this case the vertical residuals obtained were at the level of a few centimetres). The different vertical residuals for the

Table 8. Horizontal and vertical residuals and point position errors for “sewer manholes and their elements” object class

point	$\|dX\|$ [m]	$\|dY\|$ [m]	$\|dH\|$ [m]	mP_i [m]
KAN1	0.011	0.008	0.002	±0.014
KAN10	0.019	0.019	0.002	±0.027
KAN13	0.005	0.027	0.003	±0.027
KAN2	0.010	0.043	0.002	±0.044
KAN5	0.022	0.016	0.002	±0.027
KAN6	0.018	0.018	0.001	±0.025
KAN3	0.049	0.008	0.001	±0.050
KAN11	0.011	0.063	0.008	±0.064
KAN15	0.008	0.013	0.050	±0.015
KAN17	0.063	0.039	0.019	±0.074
KAN18	0.045	0.037	0.010	±0.058
KAN19	0.051	0.057	0.015	±0.076
KAN25	0.023	0.032	0.028	±0.039
KAN4	0.043	0.021	0.017	±0.048
KAN9	0.024	0.010	0.019	±0.026
Mean	0.033	0.033	0.018	±0.050

"sewer manholes and their elements" object class are presented in the penultimate column of Table 8 below. In the last column values of mP_i error were calculated on the basis of formula 8.

According to accuracy requirements, "height objects" like sewer manholes should be measured with ±3 mm accuracy. Table 8 presents that not all these elements are accurate enough. It is related strictly to the distance (and in consequence) to the resolution of point clouds representing such elements. Seven of fifteen sewer manholes could be identified and determined with required accuracy. These manholes were located on the roads and pavements, being on the mobile platform route. In table 8 manholes are placed ascending according to accuracy (first seven manholes – figure App2 are these close to the mobile laser scanning instrument).

Apart from sewer manholes, a similar phenomenon was noted in the case of pavement curbs, sewage grates, and other road infrastructure objects. This means that for objects located on the roads (including for the road surface) and in the immediate vicinity of roads, low residuals and vertical values are obtained. Additionally, taking into account the fact that an MLS point cloud for road infrastructure objects meets the accuracy requirements for the 1st accuracy group for situational elements, it can be concluded that an MLS point cloud constitutes one of the most important sources of spatial data for the needs of creating documentation for the purposes of modernising the road network, road routes inventories, creating cross-sections and longitudinal profiles of roads.

Included in Table 7 is the "road cross-sections" class. While for the road infrastructure elements discussed above low vertical error values were obtained, the root mean square error for the "road cross-sections" amounted to $RMSE_H = \pm 0.060$ m. Individual points of cross-sections should be determined with high accuracy, because thanks to them it is possible to obtain information on the direction of water flow during rain, as well as to check whether there are any places where water can accumulate. In practice, the error value would make it impossible to use the MLS data for producing cross-sections. Nevertheless, it should be noted that it would be very time-consuming to develop cross-sections for a long road stretch by means of classic surveying measurements.

5. Conclusions

Today's navigation systems and mobile remote sensing systems which allow the fast acquiring object's points are slowly displacing analogue and numerical maps produced by traditional methods. Conducted analysis confirmed that mobile laser scanning systems can be applied in some geodetic applications, especially in actualization or production of base-map. The proposed OPE_{MSL} values are close to the $RMSE$ values calculated on the basis of reference measurements. That means, it may be used in the future as no-reference metric of the accuracy evaluation. The advantage of the developed accuracy index is the ability to determine it without reference measurements, knowing the system parameters and the resulting point clouds.

The majority of object classes are characterised of a horizontal accuracy of ±0.060 m. The smallest accuracy was noted in the "trees" object class. Also the highest height error ($RMSE_H$) was noted for the "building corners" class, with the value of ±0.073 m. This error value was due to i.a. inaccessibility of a given element, in which case the lowest visible point was measured. Nevertheless, the most important conclusion is related to elements that require accuracy height measurements (like manholes). It is possible to acquire MLS point clouds with satisfying accuracy but, there is significant resolution condition, dictated by the distance from the object. If we would like to ensure the required accuracy of height measurements (±3 mm for manholes), MLS measurements should be taken at a distance of not more than 5 m, or if necessary, leveling supplementary measurements could be made. Knowing scanning parameters instead of reference measurements, OPE_{MSL} index can be used.

Further analysis will focus on comparison of terrestrial, georeferenced static scanners application with mobile systems in generating other geodetic products and applications like accurate 3D models of small areas or using laser scanning measurements in structure deformation analysis.

Acknowledgement

The research has been conducted with the frame of research at the Military University of Technology, Faculty of Civil Engineering and Geodesy.

References

Bakula, K., Dominik, W. and Ostrowski, W. (2015). Enhancement of Lidar Planimetric Accuracy using Orthoimages. *Photogrammetrie Fernerkundung Geoinformation*, (2), 143–155. DOI: 10.1127/pfg/2015/0260.

Bobkowska, K., Przyborski M., Szulwic, J. and Janowski, A. (2016). Analysis of High Resolution Clouds of Points as a Source of Biometric Data. In 2016 BALTIC GEODETIC CONGRESS (BGC GEOMATICS), 2–4 June 2016 (pp. 15–21), Gdansk, Poland. DOI: 10.1109/BGC.Geomatics.2016.12.

Fryskowska, A. (2017). Accuracy Assessment of Point Clouds Geo-Referencing in Surveying and Documentation of Historical Complexes. In 2017 GEOMATICS & RESTORATION – Conservation of Cultural Heritage in the Digital Era, 22–24 May 2017. *The International Archives of the Photogrammetry, Remote Sensing and Spatial Information Sciences*, XLII-5(W1), (pp. 161–165), Florence, Italy. DOI: 10.5194/isprs-archives-XLII-5-W1-161-2017.

Fryskowska, A., Walczykowski, P., Delis P. and Wojtkowska, M. (2015). ALS and TLS data fusion in cultural heritage documentation and modeling. In 25th International CIPA Symposium 2015, 31 August – 04 September 2015. *International Archives of the Photogrammetry Remote Sensing and Spatial Information Sciences*, XL-5(W7), (pp. 147–150). Taipei, Taiwan. DOI: 10.5194/isprsarchives-XL-5-W7-147-2015.

Gandolfi, S., Barbarella, M., Ronci, E. and Burchi, A. (2008). Close photogrammetry and laser scanning using a mobile mapping system for the high detailed survey of a high density urban area. In 3D Virtual Reconstruction and Visualization of Complex Architectures, 25–27 February 2015. *International Archives of the Photogrammetry, Remote Sensing and Spatial Information Sciences*, XXXVII(B5), (pp. 909–914). Avila, Spain.

García-San-Miguel, D. and Lerma, J.L. (2013). Geometric calibration of a terrestrial laser scanner with local additional parameters: An automatic strategy. *ISPRS Journal of Photogrammetry and Remote Sensing*, 79, 122–136. DOI: 10.1016/j.isprsjprs.2013.02.007.

Glowienka, E., Michalowska, K., Opalinski P., Hejmanowska, B., Mikrut, S. and Kramarczyk, P. (2017). Use of LIDAR Data in the 3D/4D Analyses of the Krakow Fortress Objects. In IOP Conference Series-Materials Science and Engineering, (245), article Number: UNSP 042080. DOI: 10.1088/1757-899X/245/4/04.

Hebert, M. and Krotkov, E. (1992). 3D measurements from imaging laser radars: how good are they? *Image and Visual Computation*, 10 (3), 170–178. DOI: 10.1016/0262-8856(92)90068-E.

Iavarone, A. (2002). Laser Scanning Fundamentals. *Profesional Surveying Magazine*, 22(9), retrieved 3 January, 2018, from http://www.profsurv.com/magazine/article.aspx?i=949.

Jenerowicz, A. and Siok, K. (2017). Fusion of radar and optical data for mapping and monitoring of water bodies. In SPIE Remote Sensing Proceedings, 2 November 2017 (10421/XIX pp. 261–269), Warsaw, Poland. DOI: 10.1117/12.2278365.

Kaartinen H., Hyyppä J., Kukko A., Lehtomäki M., Jaakkola A., Vosselman G., Elberink S.O., Rutzinger, M., Pu, Shi and Vaaja, M. (2013). Mobile Mapping – Road Environment Mapping using Mobile Laser Scanning, European Spatial Data Research. *EuroSDR – European Spatial Data Research*, 62, 49–95.

Kaartinen, H., Hyyppä, J., Kukko A., Jaakkola A. and Hyyppä, H. (2012). Benchmarking the Performance of Mobile Laser Scanning Systems Using a Permanent Test Field. *Sensors*, 12 (9), 12814–12835, DOI: 10.3390/s120912814.

Kedzierski, M., Fryskowska, A., Wierzbicki, D., Dabrowska, M. and Grochala, A. (2015). Impact Of The Method Of Registering Terrestrial Laser Scanning Data On The Quality Of Documenting Cultural Heritage Structures. In 25th International CIPA Symposium 2015, 31 August–04 September 2015. *International Archives of the Photogrammetry Remote Sensing and Spatial Information Sciences*, XL-5(W7), (pp. 245–248), DOI: 10.5194/isprsarchives-XL-5-W7-147-2015.

Lee, D.T., Schachter, B.J. (1980). Two Algorithms for Constructing a Delaunay Triangulation. *International Journal of Computer and Information Sciences*, 9 (3), 219–242.

Lenda, G., Marmol U. and Mirek, G. (2015). Accuracy of Laser Scanners for Measuring Surfaces made of Synthetic Materials. *Photogrammetrie Fernerkundung Geoinformation*, 5, 357–372, DOI: 10.1127/pfg/2015/0273.

Lichti, D., Gordon, S. and Tipdecho, T. (2005). Error Models and Propagation in Directly Georeferenced Terrestrial Laser Scanner Networks. *Journal Surveying Engineering* 1, 135–142.

Lichti, D. and Gordon, S.J. (2004). Terrestrial laser scanners with a narrow field of view: the effect on 3D resection solutions. *Survey Review* 37(292), 448–468. DOI: 10.1179/sre.2004.37.292.448.

Lin, Y., Hyyppä, J., Kaartinen, H. and Kukko, A. (2013). Performance Analysis of Mobile Laser Scanning Systems in Target Representation. *Remote Sensing 5*, 3140–3155. DOI: 10.3390/rs5073140.

Lubczonek, J. (2016). Location Determination of Radar Sensors by Using LIDAR data. In Conference: 17th International Radar Symposium (IRS), 10–12 May 2016 (Accession Number: 16104485). Krakow, Poland. DOI: 10.1109/IRS.2016.7497289.

Markiewicz, J. and Zawieska, D. (2015). Quality assessment of the TLS data in conservation of monuments, In SPIE Remote Sensing Proceeedings, 30 June 2015 (pp. 95270V-1-10), Munich, Germany, DOI: 10.1117/12.2184911.

Mikrut, S., Kohut, P, Pyka, K., Tokarczyk, R., Barszcz, T. and Uhl, T. (2016). Mobile Laser Scanning Systems for Measuring the Clearance Gauge of Railways: State of Play, Testing and Outlook. *Sensors*, 16 (5), Article Number: 683, DOI: 10.3390/s16050683.

Osada, E., Sosnica, K., Borkowski, A., Owczarek-Wesolowska, M. and Gromczak, A. (2017). A Direct Georeferencing Method for Terrestrial Laser Scanning Using GNSS Data and the Vertical Deflection from Global Earth Gravity Models. *Sensors*, 17 (7), Article Number: 1489, DOI: 10.3390/s17071489.

Poręba, M. and Goulette, F. (2012). Assessing the Accuracy of Land-Based Mobile Laser Scanning Data. *Geomatics And Environmental Engineering*, 6 (3), 73–81. DOI: 10.7494/geom.2012.6.3.73.

Regulation in base map production. (2011). Rozporządzenie Ministra Spraw Wewnętrznych i Administracji z dnia 9 listopada 2011 r. w sprawie standardów technicznych wykonywania geodezyjnych pomiarów sytuacyjnych i wysokościowych oraz opracowywania i przekazywania wyników tych pomiarów do państwowego zasobu geodezyjnego i kartograficznego. Poland.

Reshetyuk, Y. (2010). Direct Georeferencing with GPS in Terrestrial Laser Scanning, ZFV – Zeitschrift fur Geodasie. *Geoinformation und Landmanagement*, 135 (3), 151–159.

Reshetyuk, Y. (2009). *Self-calibration and direct georeferencing in terrestrial laser scanning*. Doctoral dissertation, Royal Institute of Technology (KTH), Stockholm, Sweden.

dos Santos, D.R., Dal Poz, A.P. and Khoshelham, K. (2013). Indirect Georeferencing of Terrestrial Laser Scanning Data using Control Lines. *Photogrametric Record*, 28, 276–292. DOI: 10.1111/phor.12027.

Scaioni, M. (2005). Direct georeferencing of TLS in surveying of complex sites. In: Proceedings of the ISPRS Working Group V/4 Workshop 3D-ARCH, Virtual Reconstruction and Visualization of Complex Architectures, August 22–24, Mestre-Venice, Italy: http://www.isprs.org/ publications/archives.html.

Shan, Jie, Toth, Ch.K. (2009). *Topographic Laser Ranging And Scanning – Principles And Processing*, Boca Raton 2009, CRC Press Taylor & Francis Group.

Sloan, S.W. (1987). A fast algorithm for constructing Delaunay triangulations in the plane, *Advances in Engineering Software.*, 9 (1), 34–55. DOI: doi.org/10.1016/0141-1195(87)90043-X.

Toschi, I., Rodríguez-Gonzálvez, P., Remondino, F., Minto, S., Orlandini, S. and Fuller, A. (2015). Accuracy Evaluation of a Mobile Mapping System with Advanced Statistical Methods. In 3D Virtual Reconstruction and Visualization of Complex Architectures. 25-27 February 2015, *International Archives of the Photogrammetry, Remote Sensing and Spatial Information Sciences*, XL-5/W4, (pp. 245–253). Avila, Spain. DOI: 10.5194/isprsarchives-XL-5-W4-245-2015.

Wilinska, M., Kedzierski, M., Zaplata, R., Fryskowska, A. and Delis, P. (2012). Noninvasive Methods Of Determining Historical Objects Deformation Using TLS. In Conference: 8th International Conference on Structural Analysis of Historical Constructions, *Structural Analysis of Historical Constructions*, 1–3, 2582–2588.

Woroszkiewicz, M., Ewiak I. and Lulkowska, P. (2017). Accuracy assessment of TanDEM-X IDEM using airborne LiDAR on the area of Poland. *Geodesy and Cartography*, 66 (1), 137–148, DOI: 10.1515/geocart-2017-0007.

Zacharek, M., Delis, P., Kedzierski, M. and Fryskowska, A., (2017). Generating Accurate 3d Models Of Architectural Heritage Structures Using Low-Cost Camera And Open Source Algorithms. In 2017 GEOMATICS & RESTORATION – Conservation of Cultural Heritage in the Digital Era, 22–24 May 2017, *The International Archives of the Photogrammetry, Remote Sensing and Spatial Information Sciences*, XLII-5(W1), (pp. 99–104), Florence, Italy. DOI: 10.5194/isprs-archives-XLII-5-W1-99-2017.

http://bandwork.my/product/54/Topcon-GPT-3100N.html#.Wj0V0jfdhPY.

http://www.leica-geosystems.pl/pl/Leica-Sprinter-150M-250M_5284.htm.

http://www.laser-3d.pl/skanery/skanery-riegl/skanowanie-mobilne-rriegl/riegl-vmx-250.

http://hds.leica-geosystems.com/downloads123/hds/hds/ScanStation/brochures-datasheet/Leica_Scan Station%202_datasheet_en.pdf.

Appendix 1.
Examples of the elements and reference data points in one of the areas

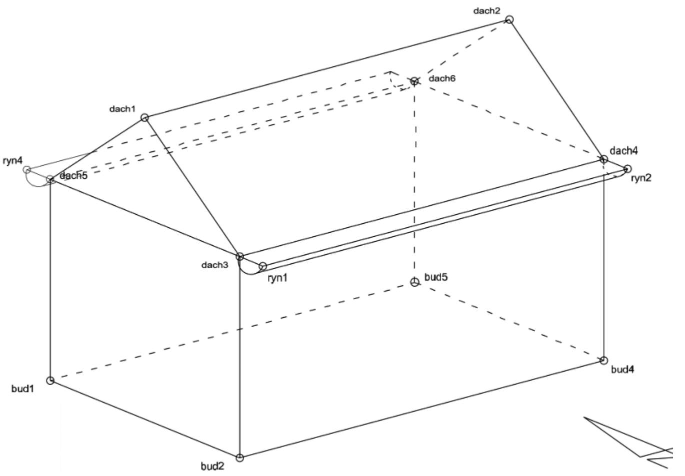

Fig. A1. Examples of reference points

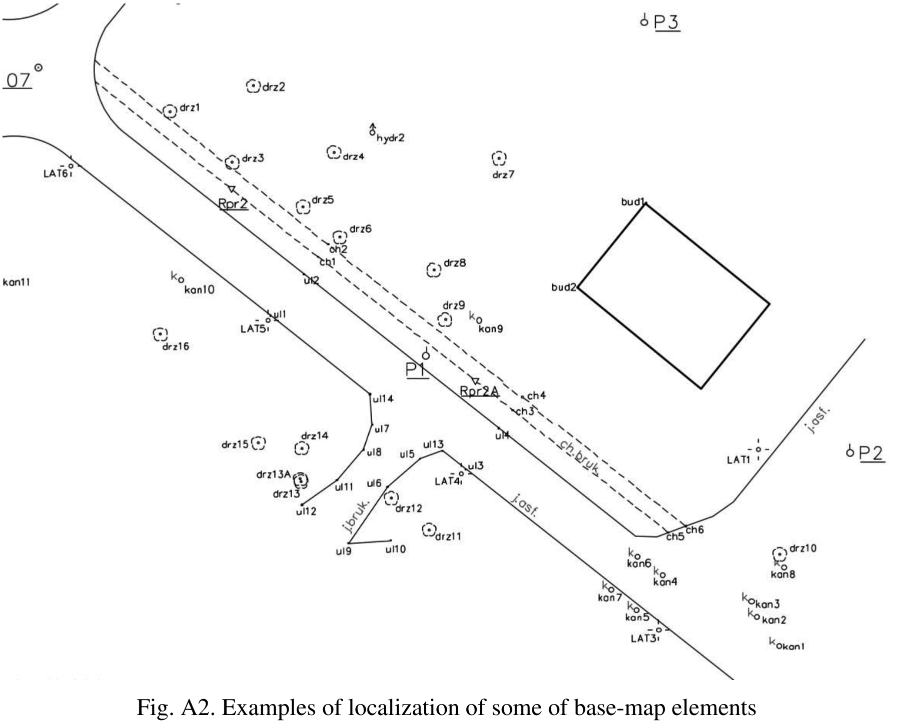

Fig. A2. Examples of localization of some of base-map elements